ACADEMIA JOURNAL OF BIOLOGY 2025, 47(4): 73–85
DOI: 10.15625/2615-9023/22493

DELETION OF YEAST *YCA1* GENE INHIBITS MITOCHONDRIAL RESPIRATORY COMPLEX ACTIVITY AND INDUCES APOPTOSIS

Van Ngoc Bui[1,2,*], Duc Duy Nguyen[1,]

[1]Institute of Biology, Vietnam Academy of Science and Technology, 18 Hoang Quoc Viet, Ha Noi, Vietnam
[2]Graduate University of Science and Technology, Vietnam Academy of Science and Technology, 18 Hoang Quoc Viet, Ha Noi, Vietnam

Received 11 June 2025; accepted 5 December 2025

ABSTRACT

Mitochondria play a central role in energy metabolism and the respiratory chain. They also play a major role in programmed cell death or apoptosis. Reactive oxygen species (ROS) are generated through both exogenous and endogenous pathways and pose a significant damage to DNA, lipids, and protein. Mitochondrial DNA (mtDNA) damage could result in loss of expression of mitochondrial polypeptides, inhibition of mitochondrial activity, induction of apoptosis. Thus, the purpose of the present study is to investigate the role of the *YCA1* gene by using the BY4741 (wild type) and specific knock-out yeast strains (Δ*yca1*). The activity of this gene in the mitochondrial respiratory chain and cellular apoptosis in response to DNA damage triggered by methyl methanesulfonate (MMS) treatment would be elucidated by using flow cytometry, chromatography, and OxoPlate® assay.

The findings indicated that fully functional yeast caspase-1 encoded by *YCA1* significantly attenuates the intracellular ROS level, while deletion of *YCA1* (Δ*yca1*) results in gradual ROS accumulation upon MMS treatment, thereby introducing damage to mtDNA, leading to inhibition of mitochondrial activity and oxygen consumption. Subsequently, the absence of *YCA1* leads to blockage in the mitochondrial electron transport chain (mtETC), repression of ATP synthesis, and fluctuation of cellular energy status (AEC). Altogether, high mitochondrial activity of the wild type acts as a protective mechanism against oxidative stress (ROS), whereas low mitochondrial activity of the Δ*yca1* enhances susceptibility to ROS that strongly induce apoptosis. These findings suggest that fully functional *YCA1* plays a major role in the protection of cell from DNA damage, while mutation of the *YCA1* gene results in a reduction of the living mutant Δ*yca1* cells accompanied with cell nucleic apoptosis.

Keywords: Apoptosis, ATP, DNA damage, mitochondria, ROS, *YCA1*.

Citation: Van Ngoc Bui, Duc Duy Nguyen, 2025. Deletion of yeast *YCA1* gene inhibits mitochondrial respiratory complex activity and induces apoptosis. *Academia Journal of Biology*, 47(4): 73–85. https://doi.org/10.15625/2615-9023/22493

[*]*Corresponding author email*: bui@ibt.ac.vn

INTRODUCTION

Like mammalian cells, yeast cells can undergo cell death accompanied by cellular markers of apoptosis. Cell death with apoptosis-like features has also been reported in yeast after treatment with formic acid, UV-irradiation, glutathione-depleting chemicals and hydrogen peroxide (H_2O_2) (Du et al., 2008; Greetham et al., 2013; Wang et al., 2014). The common denominator in most of these cell-death models that involve yeast seems to be an accumulation of reactive oxygen species (ROS). A caspase-like protein with homology to mammalian caspases has been identified in *Saccharomyces cerevisiae* (Yor197w) and implicated in cell death that is induced by H_2O_2, acetic acid and ageing (Lee et al., 2007; Madeo et al., 2002). This protein is called yeast caspase-1 (*YCA1*) and is a member of the metacaspase family - putative proteases that have a caspase-like folding. Overexpression of *YCA1* enhances apoptosis-like death of yeast that is induced by H_2O_2 or acetic acid, whereas excision of the *YCA1*-encoding gene reduces cell death (Lam & Sherlock, 2023). Furthermore, the *YCA1* protein also seems to undergo proteolytic processing in an active-site cysteine dependent-manner, which is similar to mammalian caspases (Khan et al., 2005; Mazzoni & Falcone, 2008).

In yeast, Yca1 and Aif1 (apoptosis inducing factor), encoded by the *YCA1* and *AIF1* genes are important components in yeast apoptosis in response to DNA damage (Amigoni et al., 2016; Muzaffar & Chattoo, 2017). Yca1, a member of the metacaspase family, plays a crucial role in the regulation of yeast apoptosis. When cells are exposed to oxidative stress (ROS) or DNA damaging agents, cytochrome c is released from mitochondria to the cytosol (along with other proteins such as Aif1), which activates Yca1 to induce apoptosis (Muzaffar & Chattoo, 2017; Wang et al., 2014). Furthermore, oxidative damage generated by intracellular ROS can lead to DNA base modification, single- and double-strand breaks (Canete, Andrés, et al., 2023). Thus, cells defective in *YCA1* could result in the influence of cell death or apoptosis in response to DNA damage.

The budding yeast *S. cerevisiae* has long been recognized as a versatile model system for drug discovery and studying of cellular defense in eukaryotic cells, since many of the basic cellular processes of both yeast and humans are also highly conserved. However, to date, no comprehensive analysis has yet been conducted to investigate the role of the *YCA1* gene in the attenuation of intracellular ROS level, mitochondrial respiration and activity, and apoptosis induction in response to DNA damage induced by DNA damaging agent.

Thus, the aim of this study is to investigate whether mutation of the *YCA1* gene would lead to intracellular ROS generation, mitochondrial complex activity, and apoptosis in *S. cerevisiae*. The present study, therefore, uses the model yeast strain BY4741 (wild type) and the mutant Δ*yca1* that is defective in the *YCA1* gene deleted by the disruption of the respective gene to test these assumptions.

MATERIALS AND METHODS

Strains, media and growth conditions

The two yeast strains *S. cerevisiae* used in this study are BY4741 wild type (Accession number: Y00000; Genotype: *MATα; his3Δ1; leu2Δ0; lys2Δ0; ura3Δ0*; Source: EUROSCARF) and the mutant Δ*yca1* (Accession number: Y02453; Genotype: *MATα; his3Δ1; leu2Δ0; lys2Δ0; ura3Δ0; YOR197w:kanMX4*; Source: EUROSCARF). Yeast cells were grown in rich medium (YPD, Yeast Peptone Dextrose) containing 10 g/L yeast extract, 20 g/L bacto peptone, and 20 g/L glucose. Cell growth was followed by optical absorbance measurement at 600 nm (OD_{600}). For treatment with DNA-damaging agents, e.g. methyl methanesulfonate (MMS), medium was inoculated from an overnight preculture and grown at 30 ˚C to the mid-log phase (OD_{600} 0.6–0.8). Then, cultures were either untreated (control) or treated with different concentrations of MMS (Sigma-Aldrich).

Detection of ROS level and mitochondrial activity by flow cytometry

Preparation: Yeast cells were inoculated in YPD medium, incubated at 30 ºC/250 rpm/overnight (pre-culture), then the pre-culture was transferred in fresh YPD, incubated at 30 ºC/250 rpm until mid-log phase (main culture). The main culture was split into two, one half culture as control (non-treated), and another one was treated with 0.03% MMS. Aliquots (ca 50–100 µL) were taken at 3, 6, 8 and 24 h after MMS treatment and mixed with ca 900 µL PBS (ca 1 mL total). Aliquots were either stained with 50 µM dihydroethidium (DHE, Molecular Probes, in final concentration - in f.c) for ROS detection or stained with 1 µM MitoTracker® Green FM (Molecular Probes - in f.c) plus 5 µg/mL of propidium iodide (PI, Sigma-Aldrich, in f.c) for mitochondrial activity detection. For apoptosis analysis, the annexin V/PI staining assay (BD Biosciences, Germany) was used to analyze cell apoptosis according to the protocol of the manufacturer. Living cells were determined as cells negative for both V and PI (V−/PI−), early apoptosis as cells positive for annexin V but negative for PI (V+/PI−), late apoptosis as cells positive for both annexin V and PI (V+/PI+), and necrotic cells as cells negative for V but positive for PI (V−/PI+). An aliquote of the resuspended cells was used to determine the cell number after treatment, using a hemocytometer and trypan blue. The relative amount of cells was calculated as the number of trypan blue negative cells divided by the number in the mock treatment (Bui et al., 2024).

Flow cytometry analysis (FACS): FACS® Calibur (Becton Dickinson) and CellQuest Pro analysis software were used to quantified and analyzed fluorescence intensity of DHE, PI-DNA complex (excitation and emission settings were 488 and 564–606 nm, FL2 filter), and MitoTracker® (excitation and emission settings were 488 and 525–550 nm, FL1 filter). Fluorescence intensity indicates the presence and quantity of a fluorescent marker, called relative fluorescence. Also, it refers to the proportion of cells in a sample and is calculated by dividing the number of fluorescent cells by the total number of events (relative cell number) in the sample. Thus, the fluorescence signal was proportional to ROS level and mitochondrial activity, respectively. The analyzed fluorescence signal was given in the mean value of fluorescence intensity at the indicated time point (time course).

OxoPlate® Assay

OxoPlate® (PreSens, Germany) was used to monitor oxygen consumption during yeast cell growth in medium. Yeast cells were first inoculated in YPD medium, incubated at 30 ºC/250 rpm/overnight (pre-culture), then the pre-culture was transferred into fresh respective media YPD (main culture). Oxygen consumption (%) and cell growth ($OD6_{00}$) were monitored in 96-well OxoPlate® with round bottom integrated optical oxygen sensors, in which each well contained 75 µL of adjusted main culture (0.1 OD_{600}) and 75 µL of MMS with investigated concentration (i.e. 150 µL total). The OxoPlate® was sealed with a breathable membrane (Diversified Biotech, USA), then introduced to the Tecan Safire^2 Reader (Tecan, Switzerland) to measure fluorescence intensity at 540/650 nm (for indicator dye, $I_{indicator}$) and 540/590 nm (for reference dye, $I_{reference}$), and at 600 nm (for optical density of culture, OD_{600}). The measurement was carried out continuously over 18 h with a kinetic interval of 30 min at 30 ºC. The calibration of the fluorescence reader was performed using a two-point calibration curve with oxygen free water (80 mM Na_2SO_3, *Cal 0*) and air-saturated water (*Cal 100*). Partial pressure of oxygen was calculated from the calibration curve.

Analysis of nucleotide content by HPIC

Metabolite extraction and sample preparation: The sampling preparation was described previously (Loret et al., 2007). Briefly, 20 units OD_{600} of cell culture were withdrawn at the indicated time point, rapidly collected by vacuum filtration (Glass Filter, Millipore™) through a Sartolon polyamide membrane (Sartorius, Germany). Cell-adherent membrane was quenched in 5 mL buffered

ethanol (75% ethanol, 10 mM Hepes, pH 7.1) in a 50 mL-glass tube (Lenz, Laborglas-instruments, Germany), shortly vortexed, incubated at 85 ºC/4 min in a water bath, and immediately put on ice. The membrane was then washed 2 × 0.5 mL with absolute ethanol to rinse the rest on the membrane in the solvent. The solvent containing cell extract suspension was evaporated to dryness at 35–40 ºC under vacuum in a rotary evaporator around 35–50 mbar (Büchi, Rotavapor R, Switzerland). Cell extract was resuspended in 0.5 mL deionized water, centrifuged at 1,3000 rpm/4 ºC/5 min. Supernatant was introduced to HPIC for analysis.

Analysis of nucleotide content: Supernatants (ca 200 µL) were transferred into 1.5 mL-screw thread vials with glass inserts (VWR™) and analyzed by High Performance Ion Exchange Chromatography (HPIC, Dionex - ICS - 3000, USA) equipped with a gradient pump and conductivity detector, along with a UV detector (wavelength was set either to 220 or 260 nm). For the chromatographic separation, an AG11 guard column (50 mm × 2 mm i.d.) and 2 AS11 analytical columns (250 mm × 2 mm i.d.) (Dionex) in series were used. A flow of 0.35 ml/min was maintained throughout all runs. Suppressor current was set to 70 mA. The sample injection volume was 5 µL. The data was analyzed by Chromeleon software (Dionex, ICS - U3000). The content of metabolites and nucleotides was then quantified by Chromeleon software based on the calibration curve and calculated in µmol/g DW (dry weight). The analytical protocol follows the method described in Ritter (2006) (Ritter et al., 2006).

Calculation of energy charge: Energy charge, also called adenylate energy charge (AEC), is defined as the sum of hydrolysable phosphate bonds in adenine nucleotides over the total concentration of these nucleotides. Adenylate energy charge (AEC) is an index to estimate the cell energy status and is calculated as proportional to the mole fraction of ATP plus half the mole fraction of ADP (Atkinson, 1968). The value of nucleotide levels was calculated in µmol/g DW and total intracellular adenine nucleotides AXP = (ATP + ADP + AMP). AEC was calculated as equal to (ATP +1/2ADP)/(ATP + ADP + AMP).

Statistical data analysis

Values are means of three determinations. The differences between the means were determined by Duncan's Multiple Range Test (MRT) using SAS 9.0 software (SAS Institute, Cary, NC, USA) and means with the same letter are not significantly different ($p < 0.05$). Also, one-way ANOVA and Kruskal–Wallis test were performed to determine differences in distributions between two or more independent groups using *kruskal.test* function in R, p-values < 0.05 were considered to be significantly different.

RESULTS

Intracellular ROS accumulation

ROS generation in cells treated with genotoxic chemical (MMS) is represented in Figure 1. ROS levels of all MMS-treated cultures gradually increased during cultivation until 24 h. However, ROS levels of control cultures dramatically increased at around 6–8 h during log-phase, reaching a maximum at 8 h, then starting to decrease until the end of cultivation (Fig. 1). Deletion of the *YCA1* gene (the mutant Δ*yca1*) led to gradual ROS accumulation during cultivation. Nevertheless, Δ*yca1* cells generated lower ROS levels in both control and MMS-treated cultures as compared with the BY4741 wild type (Fig. 1).

Inhibition of oxygen consumption and cell growth

The percentage of oxygen consumed over time (hours) together with cell growth expressed as OD_{600} were monitored and represented in Figure 2. The results indicate that DNA damage triggered by treatment with MMS caused adverse impairment of mitochondrial function of cells grown resulting in strong and rapid inhibition of oxygen consumption and cell growth at all investigated concentrations, especially in mutant Δ*yca1* cells. MMS treatment significantly slowed oxygen consumption and cell proliferation in a dose-dependent manner (Fig. 2).

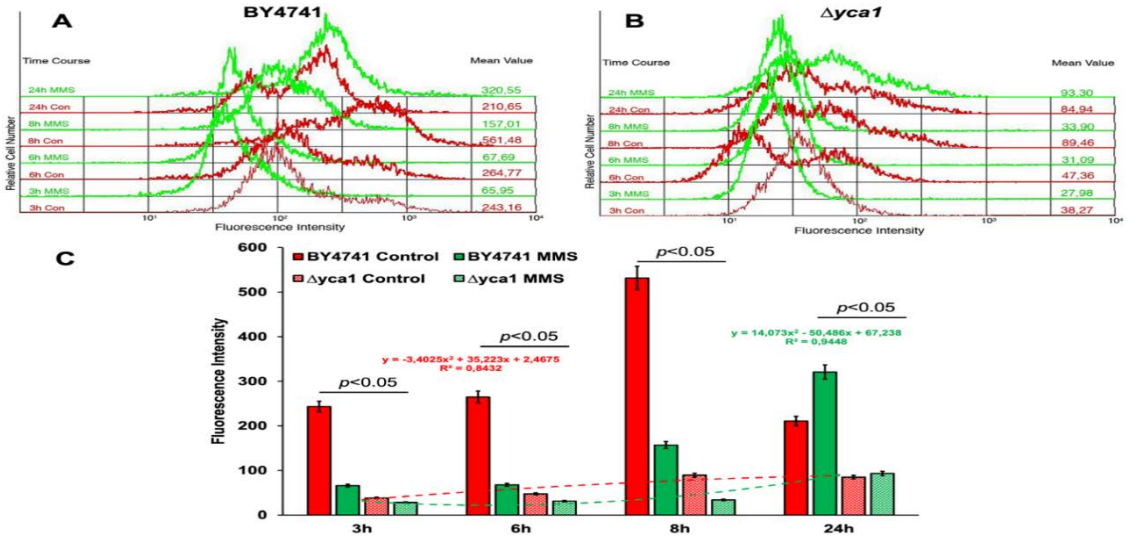

Figure 1. ROS accumulation of BY4741 (A) and Δ*yca1* (B) in response to DNA damage. Fluorescence intensity of dihydroethidium was quantified and analyzed by FACS for determining the ROS level. A and B are kinetic graphs displayed as overlapping histograms of fluorescence intensity against relative cell number. The dashed lines with quadratic equations represent the trends of ROS accumulation during 24 h of cultivation (C). Results are given as mean values with standard deviations (SD). The differences between the means were analyzed by one-way ANOVA

Afterward mitochondrial respiration was either recovered until oxygen in the medium became exhausted or remained inhibited, i.e. no more oxygen was consumed. Mutant Δ*yca1* cells were much more susceptible to MMS treatment and showed stronger enhancement of mitochondrial respiratory block leading to more rapid decrease of oxygen consumption and subsequent lower exponential growth rate compared with wild types (Fig. 2). The mutant cells were not able to regain mitochondrial respiration, resume oxygen consumption, and continue cell proliferation when exposed to genotoxic chemical as the wild type could (Fig. 2B).

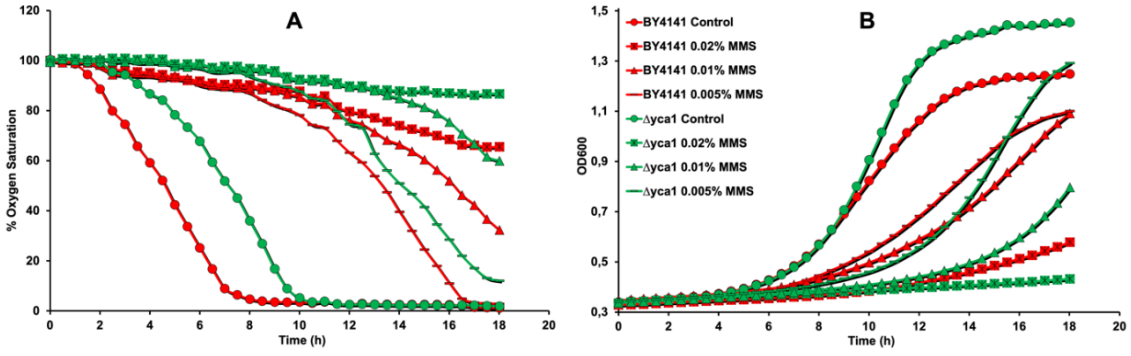

Figure 2. The kinetics of oxygen consumption (A) and cell growth (B) of the wild type BY4741 and the mutant Δ*yca1* upon treatment with MMS**.** Oxygen consumption and cell growth were monitored using a 96-well OxoPlate®. The standard deviations of measurements were less than 5%, thus omitted. The legends in the growth curves (B) are also ones in the kinetics of oxygen consumption (A)

Inhibition of mitochondrial activity

As shown in Figure 3, the mitochondrial activity of all control and MMS-treated cultures gradually decreased over the cultivation time. Additionally, the mitochondrial activity of all MMS-treated cells decreased faster than that of controls: the lower measured fluorescence intensity is the result of impairment of mitochondrial function upon MMS treatment (Fig. 3C). MMS treatment significantly reduced mitochondrial activity in a dose-dependent fashion. Mitochondrial activity of the wild type cells is higher than that of the mutant cells in both control and MMS-treated conditions. Thus, disruption of the *YCA1* gene led to inhibition of mitochondrial activity.

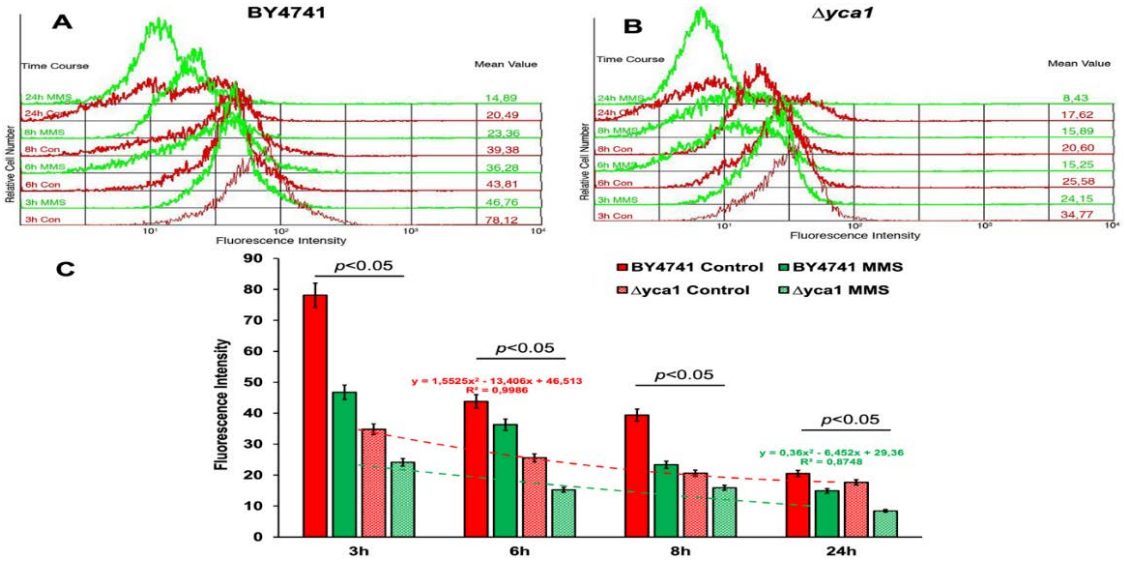

Figure 3. Modulation of mitochondrial activity of BY4741 (A) and Δ*yca1* (B) in response to DNA damage. Fluorescence intensity of MitoTracker® was quantified and analyzed by FACS for measuring mitochondrial activity. A and B are kinetic graphs displayed as overlapping histograms of fluorescence intensity against relative cell number. The dashed lines with quadratic equations represent the trends of mitochondrial activity during 24 h of cultivation (C). Results are given as mean values with standard deviations (SD). The differences between the means were analyzed by one-way ANOVA

Inhibition of ATP synthesis and energy status

The wild type BY4741 cells produced more ATP level than the mutant Δ*yca1* cells. The ATP production gradually decreased until the end of the cultivation period. MMS treatment inhibited ATP synthesis of both the wild type and Δ*yca1* already after 3 h of treatment resulting in a reduction in ATP levels as compared to controls (Figs. 4A & B). This decrease of ATP levels in MMS-treated conditions also contributed to the decrease of total adenine nucleotides (AXP) and adenylate energy charge (AEC) over time compared to controls (Figs. 4C & D).

The increase of AEC during the first hours (0–3 h) resulted from the increase of cellular ATP levels, which indicates that cells did not yet require a large number of building blocks such as amino acids and nucleotides, nor required a large amount of energy for cell proliferation. In this case, high AEC inhibits catabolism leading to a reduction of ADP and AMP levels, and a subsequent decrease in total intracellular adenine nucleotides (AXP) at this stage (Fig. 4). Thus, MMS-treated cells were not able to

maintain their energy balance as compared to untreated cells (controls). The inhibition of ATP synthesis over time contributed to the decrease of total adenine nucleotides (AXP) and subsequent adenylate energy charge (AEC) of both MMS-treated BY4741 and Δ*yca1* cells.

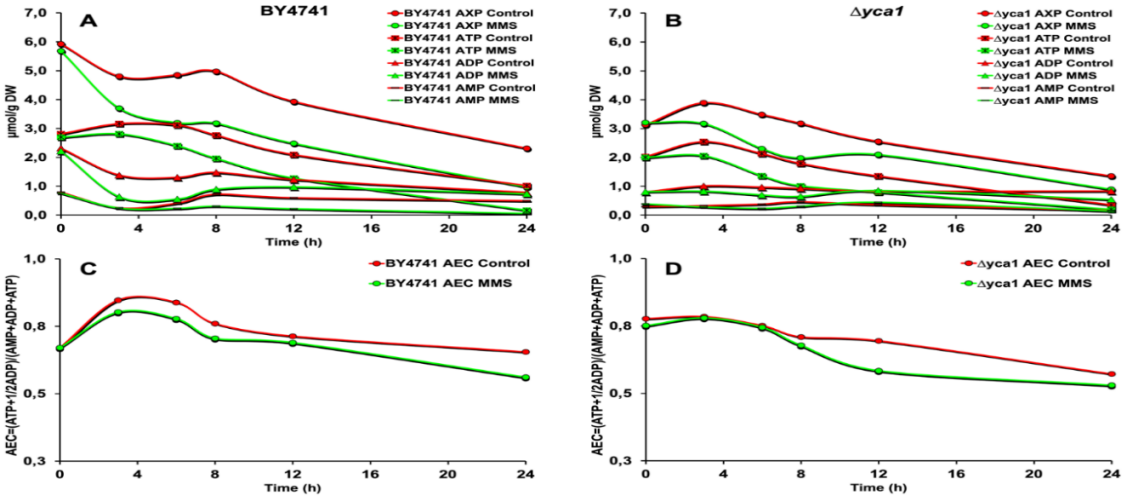

Figure 4. Changes in ATP, ADP, AMP levels and adenylate energy charge (AEC) in response to DNA damage. Intracellular metabolite extracts were analyzed by HPIC at each time point taking aliquots at 3, 6, 8, and 24 h. The value of nucleotide levels was calculated in µmol/g DW (dry weight) (panels A, B) and total intracellular adenine nucleotides AXP = (ATP + ADP + AMP). AEC was calculated as equal (ATP +1/2ADP)/(ATP + ADP + AMP) (panels C, D)

Induction of apoptosis in response to DNA damage

Apoptosis stages and apoptotic cell ratios were determined by annexin V/PI double staining, because annexin V binds to phosphatidylserine that is translocated from the inner to the outer cell membrane layer during apoptosis and PI only enters cells with damaged membrane. As demonstrated in Figure 5, MMS treatment not only reduced the relative cell number, i.e. increased the percentage of apoptotic cells, but also caused an increase in the population of cells in early apoptosis (V+/PI–), late apoptosis (V+/PI+), and necrosis (V–/PI+) as compared with the controls (Fig. 5). In other words, the number of living cells were gradually decreased, while the amount of early/late apoptotic and necrotic cells was steadily increased. The percentage of early apoptotic cells was higher than that of the late apoptotic and necrotic cells. The MMS treatment caused these effects more intensively than the control. In addition, the relative cell number of the Δ*yca1* was less than that of the BY4741 (Fig. 5).

DISCUSSION

During proliferation, eukaryotic cells are exposed to many kinds of exogenous agents like MMS and endogenous agents like ROS from oxidative metabolism that can all result in damage to DNA. MMS, an alkylating agent and carcinogen, methylates N^7-deoxyguanine and N^3-deoxyadenine bases of DNA, directly causing double-strand breaks and stalling replication forks (Groth et al., 2010; Yang et al., 2010). ROS, such as superoxide anion radical ($^*O_2^-$), hydroxyl free radicals ($^*OH$), and hydrogen peroxide (H_2O_2), are generated through both exogenous and endogenous routes and pose a significant threat to cellular integrity from damage to DNA, lipids, protein, and other macromolecules (Salmon et al., 2004). Oxidative damage generated by intracellular ROS can lead to DNA base modification, single- and double-strand breaks (Canete & Andres et al., 2023; Waterman et al., 2020).

To cope with these kinds of DNA damage, yeast cells have evolved a number of defective cellular mechanisms, including DNA damage checkpoints, cell cycle arrest, DNA damage repair (Yao et al., 2021), tolerance of DNA damage (Belli et al., 2022), and initiation of apoptosis (Mihoubi et al., 2017). *YCA1* encoded by the *YCA1* plays a crucial role in the activation of apoptosis in response to DNA damage (Du et al., 2008; Khan et al., 2005; Lam & Sherlock, 2023).

Modulation of mitochondrial respiration in response to DNA damage

In *S. cerevisiae*, the recovery of mitochondrial function and respiration, as well as the increase of cell growth, depend on the mitochondrial activity. The ATP production and energy metabolism are directly dependent on oxygen consumption. Thus, the accelerated oxygen consumption could depend on the mitochondrial activity. As compared with the wild type cells, cells lacking *YCA1* gene (Δ*yca1*) showed reduced oxygen consumption and cell growth (Fig. 2). This effect may be attributed to the high mitochondrial activity of the wild type (Fig. 3). It was able to recover mitochondrial function and regain oxygen consumption faster and increase cell survival better than the mutant (Fig. 2). The low mitochondrial activity and oxygen consumption could result from mitochondrial DNA (mtDNA) damage triggered by MMS treatment that induces high ROS accumulation and further impairs mitochondrial activity (Figs. 1–3). Since mtDNA might be more prone to oxidative damage and suffers 3–10 fold more damage than nuclear DNA (nDNA) in numerous cell types from yeast, mouse, rats, and humans (Chenna et al., 2022; Van Houten et al., 2006). Moreover, mtDNA is susceptible to ROS generated by the mitochondrial electron transport chain (mtECT). mtDNA damage can lead to loss of expression of mitochondrial polypeptides, reduction of mitochondrial activity (Shokolenko et al., 2009).

Thus, ROS levels in all MMS-treated cultures gradually accumulated over time. However, the intracellular ROS accumulation of the control cultures, especially wild type culture, was higher than that of MMS-treated cultures (Fig. 1). This could be explained that ROS is also generated by mtETC even during normal metabolism (Mendelow, 2009). Additionally, mitochondria are a source of cellular ROS as a result of electron leakage from mtETC. Leaked electrons could react with molecular oxygen to form $*O_2^-$ which is then converted to H_2O_2 at physiological pH. Electron leakage capacity correlates with mtETC activity (Gomes & Juneau, 2016; Mendelow, 2009). Also, mtDNA seems to be a critical target for such oxidative damage and is particularly susceptible to ROS generated by the mtETC due to its proximity (Senoo et al., 2016; Stenberg et al., 2022). Nevertheles, nDNA is unlikely directly damaged by H_2O_2 released from mitochondria (van Soest et al., 2024).

ROS generation, therefore, correlates with high oxygen consumption and exponential growth rate (Figs. 1–2). Our previous studies also support that mtDNA is the preferred target for MMS-mediated DNA damage and MMS treatment causes mtDNA damage, inhibition of the mtETC, and subsequent increase of ROS accumulation (Bui & Le, 2024; Kitanovic et al., 2009). The mutant Δ*yca1* mutant lacking *YCA1* indicated low mitochondrial activity (Fig. 3), leading to reduced oxygen consumption and exponential growth rate as compared with BY4741 wild type (Fig. 2). These findings suggest that fully functional Yca1 plays a crucial role in mitochondrial respiratory function.

In essence, MMS treatment could damage mtDNA, resulting in inhibition of mitochondrial respiration with a subsequent decrease of oxygen consumption but an increase of ROS level. It is possible that these also cause inhibition of ATP production and energy status.

Modulation of ATP synthesis and energy status in response to DNA damage

The ATP production and energy metabolism are directly dependent on mitochondrial respiration. Thus, low oxygen consumption and mitochondrial activity of both

the Δ*yca1* and MMS-treated cultures contributed to low ATP level and energy status (Fig. 4). Besides, many reactions in metabolism are controlled by the energy status of the cell. AEC, an index to estimate the cell energy status, is also directly dependent on AXP (Atkinson, 1968). Low AEC stimulates ATP synthesis (catabolism), but simultaneously stimulates ATP consumption (anabolism) used for DNA/RNA synthesis leading to the generation of ADP and AMP in this stage (Figs. 4A-C). It could be said that cells required a large amount of energy for exponential growth in this log-phase leading to a decrease of the cellular ATP pool. Then, AEC was nearly constant, i.e. the energy status of cells was balanced from 8 h (Fig. 4C). In other words, in this stationary phase, there is a balance between catabolism and anabolism.

Nevertheless, AEC in MMS-treated Δ*yca1* cells was strongly reduced and significantly lower than that in controls (Figs. 4C-D). The reduced AEC over time will affect the balance between catabolism and anabolism of cells. Since the AEC value reflects a balance between catabolic and anabolic pathways and depends on the relative amounts of ATP, ADP, and AMP. A high AEC value inhibits ATP synthesis, but stimulates ATP utilization and vice versa (Berg et al., 2002).

Thus, deletion of the *YCA1* gene results in damage to mtDNA leading to ROS accumulation, inhibition of mitochondrial activity, oxygen consumption, and ATP production, and impairment of cellular energy status upon MMS treatment. These effects were also observed in Δ*rad9* and Δ*hap4* cells from our earlier reports (Bui & Le, 2024; Kitanovic et al., 2009). Probably, these defects likely induce apoptosis in response to DNA damage.

Induction of apoptosis in response to DNA damage

It is well documented that mitochondria play the central role in energy metabolism and the respiratory chain; they also play an important role in programmed cell death or apoptosis (Nadalutti et al., 2020; Van Houten et al., 2006). Also, mitochondria act as "executioners" in apoptosis. Enhancement of mtDNA repair should confer protection from cell death, whereas loss of mtDNA repair should promote cell death (Leadsham & Gourlay, 2010; Lee et al., 2017; Van Houten et al., 2006).

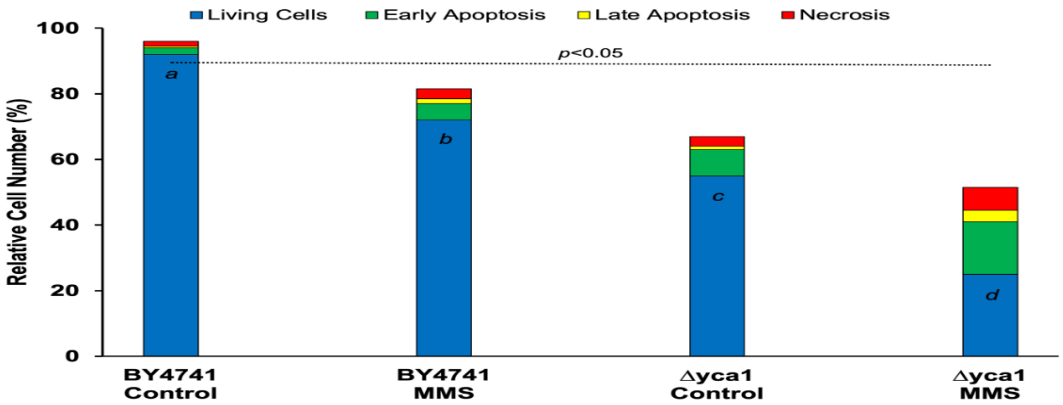

Figure 5. Induction of apoptosis in BY4741 and Δ*yca1* cells in response to DNA damage. Apoptosis stages and apoptotic cell ratios (%) were determined by FACS flow cytometry using annexin V/PI double staining and calculated by hemacytometer using trypan blue staining, respectively. All measurements were performed at least 3 times for reproducibility, and values are the means of 3 measurements. The differences between the means were analyzed by Duncan's Multiple Range Test and one-way ANOVA; means with the same letter are not significantly different ($p > 0.05$) and vice versa

Thus, all MMS-treated cells with inhibited mitochondrial respiratory function activated apoptosis in response to DNA damage. As expected, the living cells were gradually reducing, while the early/late apoptotic and necrotic cells were steadily increasing. These effects were more intensively observed in Δ*yca1* cells (Fig. 5). These findings propose that fully functional yeast caspase-1 plays a major role in the protection of the cell from DNA damage. The mutation of the *YCA1* gene leads to a reduction of the living mutant Δ*yca1* cells accompanied with nuclear apoptosis.

As above mentioned, along with *YCA1*, *AIF1* are also an important component in yeast apoptosis in response to DNA damage (Amigoni et al., 2016; Muzaffar & Chattoo, 2017). Perhaps, they interact with each other to fulfill their function in apoptosis and especially in cell cylce arrest. In addition, DNA damage causes the prohibition of mitochondrial respiratory complex activity and ATP synthesis. So, where does the carbohydrate flux (glucose) shunt to? Because it does not enter the TCA cycle and mtETC where more ATP molecules are produced. Assumably, this carbohydrate flux diverts to the hexosamine biosynthesis pathway, pentose phosphate pathway, and glycogen and trehalose synthesis. These questions and assumptions are also the limitations of the present study. Thus, further investigations will be performed in our future studies to address these questions.

CONCLUSION

Fully functional yeast caspase-1 encoded by *YCA1* significantly attenuates intracellular ROS level, while a defect of *YCA1* (Δ*yca1*) results in gradual ROS accumulation upon MMS treatment, thereby causing damage to mtDNA leading to reduced mitochondrial activity and oxygen consumption. Subsequently, lack of *YCA1* causes blockage of mtETC, repression of ATP synthesis, and fluctuation of cellular energy status (AEC). Altogether, high mitochondrial activity of the wild type acts as a protective mechanism against oxidative stress (ROS), whereas low mitochondrial activity of the Δ*yca1* enhances susceptibility to ROS that strongly trigger cellular apoptosis (Fig. 6).

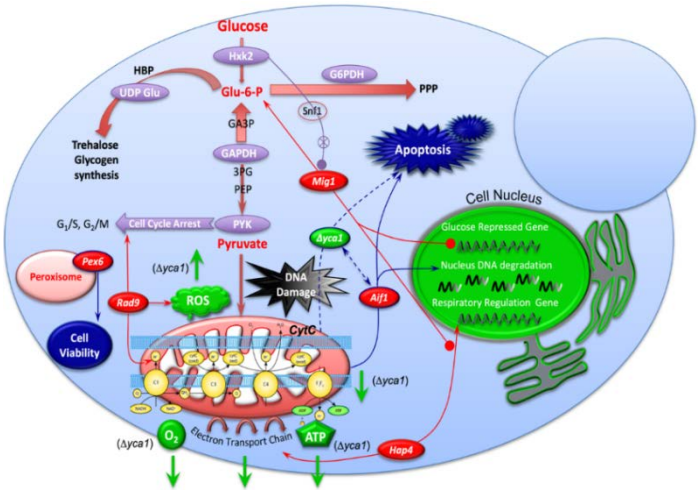

Figure 6. Schematic summary of the role of the yeast *YCA1* gene in mitochondrial respiratory complex, ATP synthesis, and apoptosis in response to DNA damage. MMS treatment strongly inhibits the mitochondrial electron transport chain-mtETC and decreases oxygen consumption and cell growth of Δ*yca1*. Further effects are the inhibition of ATP synthesis and fluctuation of AEC. Finally, cells activate cellular apoptosis as a protective mechanism, especially for cells that have low mitochondrial activity and are susceptible to intracellular ROS accumulation like Δ*yca1* cells

Acknowledgements: We thank Stefan Wölfl, Ana Kitanovic for their valuable comments regarding the experiments and for sharing ideas regarding data analysis. This work was supported by the SysMO Project Network (EU-BMBF) on Systems Biology of Microorganisms (MOSES, WP 4.3, S.W. and A.K.).

REFERENCES

Amigoni L., Frigerio G., Martegani E., Colombo S., 2016. Involvement of Aif1 in apoptosis triggered by lack of Hxk2 in the yeast *Saccharomyces cerevisiae*. *FEMS Yeast Res.*, 16(3). https://doi.org/10.1093/femsyr/fow016

Atkinson D. E., 1968. The energy charge of the adenylate pool as a regulatory parameter. Interaction with feedback modifiers. *Biochemistry*, 7(11): 4030−4034. https://doi.org/10.1021/bi00851a033

Belli G., Colomina N., Castells-Roca L., Lorite N. P., 2022. Post-translational modifications of PCNA: Guiding for the best DNA damage tolerance choice. *J. Fungi (Basel)*, 8(6). https://doi.org/10.3390/jof8060621

Berg J. M., Tymoczko J. L., Stryer L., 2002. Biochemistry, Fifth Edition: W.H. Freeman. pp. 1100.

Bui V. N., Le T. H., 2024. Regulation of yeast *RAD9* gene in energy charge, intracellular ROS, and cell cycle arrest in response to DNA damage. *Vietnam Journal of Biotechnology*, 22: 507−522. https://doi.org/10.15625/vjbt-21211

Bui V. N., Nguyen T. P. T., Nguyen H. D., Phi Q. T., Nguyen T. N., Chu H. H., 2024. Bioactivity responses to changes in mucus-associated bacterial composition between healthy and bleached *Porites lobata* corals. *J. Invertebr. Pathol.*, 206: 108164. https://doi.org/10.1016/j.jip.2024.108164

Canete J. A., Andres S., Munoz S., Zamarreno J., Rodriguez S., Diaz-Cuervo H., Bueno A., Sacristan M. P., 2023. Fission yeast Cdc14-like phosphatase Flp1/Clp1 modulates the transcriptional response to oxidative stress. *Sci. Rep.*, 13(1): 14677. https://doi.org/10.1038/s41598-023-41869-w

Canete J. A., Andrés S., Muñoz S., Zamarreño J., Rodríguez S., Díaz-Cuervo H., Bueno A., Sacristán M. P., 2023. Fission yeast Cdc14-like phosphatase Flp1/Clp1 modulates the transcriptional response to oxidative stress. *Sci. Rep.*, 13(1): 14677. https://doi.org/10.1038/s41598-023-41869-w

Chenna S., Koopman W. J. H., Prehn J. H. M., Connolly N. M. C., 2022. Mechanisms and mathematical modeling of ROS production by the mitochondrial electron transport chain. *Am. J. Physiol. Cell Physiol.*, 323(1): C69-C83. https://doi.org/10.1152/ajpcell.00455.2021

Du L., Su Y., Sun D., Zhu W., Wang J., Zhuang X., Zhou S., Lu Y., 2008. Formic acid induces Yca1p-independent apoptosis-like cell death in the yeast *Saccharomyces cerevisiae*. *FEMS Yeast Res.*, 8(4): 531−539. https://doi.org/10.1111/j.1567-1364.2008.00375.x

Gomes M. P., Juneau P., 2016. Oxidative stress in duckweed (*Lemna minor* L.) induced by glyphosate: Is the mitochondrial electron transport chain a target of this herbicide? *Environ. Pollut.*, 218: 402−409. https://doi.org/10.1016/j.envpol.2016.07.019

Greetham D., Kritsiligkou P., Watkins R. H., Carter Z., Parkin J., Grant C. M., 2013. Oxidation of the yeast mitochondrial thioredoxin promotes cell death. *Antioxid. Redox Signal.*, 18(4): 376−385. https://doi.org/10.1089/ars.2012.4597

Groth P., Auslander S., Majumder M. M., Schultz N., Johansson F., Petermann E., Helleday T., 2010. Methylated DNA causes a physical block to replication forks independently of damage signalling, O(6)-methylguanine or DNA single-strand breaks and results in DNA damage. *J. Mol. Biol.*, 402(1): 70−82. https://doi.org/10.1016/j.jmb.2010.07.010

Khan M. A., Chock P. B., Stadtman E. R., 2005. Knockout of caspase-like gene,

YCA1, abrogates apoptosis and elevates oxidized proteins in S*accharomyces cerevisiae*. *Proc. Natl. Acad. Sci. U. S. A.*, 102(48): 17326−17331. https://doi.org/10.1073/pnas.0508120102

Kitanovic A., Walther T., Loret M. O., Holzwarth J., Kitanovic I., Bonowski F., Van Bui N., Francois J. M., Wolfl S., 2009. Metabolic response to MMS-mediated DNA damage in *Saccharomyces cerevisiae* is dependent on the glucose concentration in the medium. *FEMS Yeast Res.*, 9(4): 535−551. https://doi.org/10.1111/j.1567-1364.2009.00505.x

Lam D. K., Sherlock G., 2023. Yca1 metacaspase: diverse functions determine how yeast live and let die. *FEMS Yeast Res*: 23. https://doi.org/10.1093/femsyr/foad022

Leadsham J. E., Gourlay C. W., 2010. cAMP/PKA signaling balances respiratory activity with mitochondria dependent apoptosis via transcriptional regulation. *BMC Cell Biol.*, 11: 92. https://doi.org/10.1186/1471-2121-11-92

Lee J. Y., Jun D. Y., Park J. E., Kwon G. H., Kim J. S., Kim Y. H., 2017. Pro-apoptotic role of the human YPEL5 gene identified by functional complementation of a yeast moh1delta mutation. *J. Microbiol. Biotechnol.*, 27(3): 633−643. https://doi.org/10.4014/jmb.1610.10045

Lee Y. J., Hoe K. L., Maeng P. J., 2007. Yeast cells lacking the CIT1-encoded mitochondrial citrate synthase are hypersusceptible to heat- or aging-induced apoptosis. *Mol. Biol. Cell*, 18(9): 3556−3567. https://doi.org/10.1091/mbc.e07-02-0118

Loret M. O., Pedersen L., François J., 2007. Revised procedures for yeast metabolites extraction: application to a glucose pulse to carbon-limited yeast cultures, which reveals a transient activation of the purine salvage pathway. *Yeast*, 24(1): 47−60. https://doi.org/10.1002/yea.1435

Madeo F., Herker E., Maldener C., Wissing S., Lächelt S., Herlan M., Fehr M., Lauber K., Sigrist S. J., Wesselborg S., Fröhlich K. U., 2002. A caspase-related protease regulates apoptosis in yeast. *Mol. Cell.*, 9(4): 911−917. https://doi.org/10.1016/s1097-2765(02)00501-4

Mazzoni C., Falcone C., 2008. Caspase-dependent apoptosis in yeast. *Biochim. Biophys. Acta.*, 1783(7): 1320−1327. https://doi.org/10.1016/j.bbamcr.2008.02.015

Mendelow B. V., 2009. Molecular medicine for clinicians (Second Edition ed.). Johannesburg, South Africa: Wits University Press, pp. 300.

Mihoubi W., Sahli E., Gargouri A., Amiel C., 2017. FTIR spectroscopy of whole cells for the monitoring of yeast apoptosis mediated by p53 over-expression and its suppression by *Nigella sativa* extracts. *PLoS One*, 12(7): e0180680. https://doi.org/10.1371/journal.pone.0180680

Muzaffar S., Chattoo B. B., 2017. Apoptosis-inducing factor (Aif1) mediates anacardic acid-induced apoptosis in *Saccharomyces cerevisiae*. *Apoptosis*, 22(3): 463−474. https://doi.org/10.1007/s10495-016-1330-6

Nadalutti C. A., Stefanick D. F., Zhao M. L., Horton J. K., Prasad R., Brooks A. M., Griffith J. D., Wilson S. H., 2020. Mitochondrial dysfunction and DNA damage accompany enhanced levels of formaldehyde in cultured primary human fibroblasts. *Sci. Rep.*, 10(1): 5575. https://doi.org/10.1038/s41598-020-61477-2

Ritter J. B., Genzel Y., Reichl U., 2006. High-performance anion-exchange chromatography using on-line electrolytic eluent generation for the determination of more than 25 intermediates from energy metabolism of mammalian cells in culture. *J. Chromatogr. B Analyt. Technol. Biomed. Life Sci.*, 843(2): 216−226. https://doi.org/10.1016/j.jchromb.2006.06.004

Salmon T. B., Evert B. A., Song B., Doetsch P. W., 2004. Biological consequences of

oxidative stress-induced DNA damage in *Saccharomyces cerevisiae*. *Nucleic Acids Res.*, 32(12): 3712−3723. https://doi.org/10.1093/nar/gkh696

Senoo T., Yamanaka M., Nakamura A., Terashita T., Kawano S., Ikeda S., 2016. Quantitative PCR for detection of DNA damage in mitochondrial DNA of the fission yeast *Schizosaccharomyces pombe*. *J. Microbiol. Methods*, 127: 77−81. https://doi.org/10.1016/j.mimet.2016.05.023

Shokolenko I., Venediktova N., Bochkareva A., Wilson G. L., Alexeyev M. F., 2009. Oxidative stress induces degradation of mitochondrial DNA. *Nucleic Acids Res.*, 37(8): 2539−2548. https://doi.org/10.1093/nar/gkp100

Stenberg S., Li J., Gjuvsland A. B., Persson K., Demitz-Helin E., Gonzalez Pena C., Yue J. X., Gilchrist C., Arengard T., Ghiaci P., Larsson-Berglund L., Zackrisson M., Smits S., Hallin J., Hoog J. L., Molin M., Liti G., Omholt S. W., Warringer J., 2022. Genetically controlled mtDNA deletions prevent ROS damage by arresting oxidative phosphorylation. *Elife*: 11. https://doi.org/10.7554/eLife.76095

Van Houten B., Woshner V., Santos J. H., 2006. Role of mitochondrial DNA in toxic responses to oxidative stress. *DNA Repair (Amst)*, 5(2): 145−152. https://doi.org/10.1016/j.dnarep.2005.03.002

van Soest D. M. K., Polderman P. E., den Toom W. T. F., Keijer J. P., van Roosmalen M. J., Leyten T. M. F., Lehmann J., Zwakenberg S., De Henau S., van Boxtel R., Burgering B. M. T., Dansen T. B., 2024. Mitochondrial H(2)O(2) release does not directly cause damage to chromosomal DNA. *Nat. Commun.*, 15(1): 2725. https://doi.org/10.1038/s41467-024-47008-x

Wang C. Q., Li X., Wang M. Q., Qian J., Zheng K., Bian H. W., Han N., Wang J. H., Pan J. W., Zhu M. Y., 2014. Protective effects of ETC complex III and cytochrome c against hydrogen peroxide-induced apoptosis in yeast. *Free Radic. Res.*, 48(4): 435−444. https://doi.org/10.3109/10715762.2014.885116

Waterman D. P., Haber J. E., Smolka M. B., Test T. T., 2020. Checkpoint responses to DNA double-strand breaks. *Annu. Rev. Biochem.*, 89: 103−133. https://doi.org/10.1146/annurev-biochem-011520-104722

Yang Y., Gordenin D. A., Resnick M. A., 2010. A single-strand specific lesion drives MMS-induced hyper-mutability at a double-strand break in yeast. *DNA Repair (Amst)*, 9(8): 914−921. https://doi.org/10.1016/j.dnarep.2010.06.005

Yao S., Feng Y., Zhang Y., Feng J., 2021. DNA damage checkpoint and repair: From the budding yeast *Saccharomyces cerevisiae* to the pathogenic fungus *Candida albicans*. *Comput. Struct. Biotechnol. J.*, 19: 6343−6354. https://doi.org/10.1016/j.csbj.2021.11.033